Recycling and Reuse Technology Transfer Center

http://www.rrttc.uni.edu

Formation of Aromatic Hydrocarbons through Gas Phase Ion-Molecule Reactions of C_3H_3

Publication: 1993 – 006

Michelle Hammer, Michaela Rich, Tim Burrell, Curtiss Hanson

FORMATION OF AROMATIC HYDROCARBONS THROUGH GAS PHASE ION-MOLECULE REACTIONS OF $C_3H_3^+$

Michelle D. Hammer, Michaela L. Rich, Tim Burrell, Curtiss D. Hanson

Department of Chemistry, University of Northern Iowa, Cedar Falls, IA 50614-0423

Abstract: The formation of benzene during the thermal decomposition of hydrocarbons has been attributed to the reaction of $C_3H_3^+$ with low molecular weight hydrocarbons. Fourier transform ion cyclotron resonance mass spectrometry (FT-ICR) permits direct observation of the gas phase reactions of $C_3H_3^+$ with conjugated dienes. Two forms of $C_3H_3^+$ are observed: *i)* The reactive propargyl isomer, which reacts with dienes to produce a phenyl cation, and *ii)* an unreactive cyclopropenyl isomer. The interconversion between these isomers is demonstrated under energetic conditions. Deuterium labeling experiments were utilized to postulate a mechanism for the reaction. An ionic model for the gas phase formation of benzene based on a reactive propargyl cation will be presented in this paper.

Introduction

The propargyl $C_3H_3^+$ cation (m/z 39) has been extensively studied as a precursor ion to the formation of soot in the pyrolysis of fuels and other hydrocarbons (1,2,3,4,5,6,7,8,9). Studies involving soot nucleation in flames point to an ionic mechanism, versus a neutral free radical mechanism, driving the formation of aromatic hydrocarbons. These aromatic hydrocarbons are believed to continue the transformation process from a molecular level to particulate systems to soot aggregates (1). These studies show that the propargyl $C_3H_3^+$ cation is critical to this transformation.

Although the mechanism for the formation of the propargyl cation is not known, it is found to be the dominant ion in fuel-rich hydrocarbon flames (10). Under these conditions, an electronically excited CH^* radical can react with the excess acetylene to form the $C_3H_3^+$ cation (equation 1).

$$CH^* + C_2H_2 \rightarrow C_3H_3^+ + e^- \qquad (1)$$

In addition, research conducted by Bowser and Weinberg (5) proposed the following reaction for the formation of $C_3H_3^+$ during the pyrolysis of hydrocarbons:

$$C_2 + CH_3 \rightarrow C_3H_3^+ + e^- \qquad (2)$$

Studies by Eyler et al. have involved modeling the soot particle initiation process

through reactions of $C_3H_3^+$ with acetylene and diacetylene using FT-ICR (2,3,4). Using Fourier transform ion cyclotron resonance (FT-ICR), the gas phase reactions arising during the pyrolysis of hydrocarbons can be modeled. The low pressure parameters obtained using FT-ICR slow down the reaction rate so that the reaction sequences can be more closely defined (11,12).

In these types of experiments, two forms of $C_3H_3^+$ are observed: *i)* The reactive linear propargyl cation *(l-*$C_3H_3^+$*)*, and *ii)* the unreactive cyclopropenyl cation *(c-*$C_3H_3^+$*)*(3,4). Theoretical calculations by Radom (13) show heats of formation of 293 kcal/mole for the propargyl isomer and 253 kcal/mole for the cyclopropenyl isomer. These values closely match experimental heats of formation reported by Lossing (14) of 281 kcal/mole the propargyl form and 256 ± 2 kcal/mole for the cyclopropenyl form. Based on these energy considerations, reaction 1 is exothermic by 100-150 kJ/mole for the production of the reactive propargyl $C_3H_3^+$ cation and exothermic by 200-250 kJ/mole for the production of the unreactive cyclopropenyl $C_3H_3^+$ cation. Furthermore, an energy profile reported by Wong and Radom (15) shows a significant activation energy of 97.6 kcal/mole required for rearrangement of the propargyl form to the cyclic form. It is estimated that under flame conditions that the concentration of the propargyl cation is less than 1% of the total $C_3H_3^+$ concentration (10). Therefore, the interconversion between these two isomers is clearly important to the proposed mechanism.

Although previous work has been done in the area of acetylene fuels and fuel pyrolysis (1,16,17,18,19), the same ionic process can be used to model styrene butadiene

(SBR) and poly-isoprene rubber pyrolysis (20). For example, the $C_3H_3^+$ cation is also observed as an important fragment ion in the gaseous products formed from the pyrolysis of styrene butadiene rubber (SBR) tires. A mass spectrum of gaseous products collected immediately following pyrolysis of SBR tires reveals low molecular weight species believed to be critical to the formation of aromatic hydrocarbons. Therefore, much can be learned about the mechanism driving the formation of aromatics by studying the formation rate of the phenyl cation from the gas phase reactions of $C_3H_3^+$ and small conjugated dienes such as furan and 1, 3-butadiene. An understanding of the mechanism for aromatic formation can provide a better understanding of soot nucleation to polycyclic aromatics during fuel and SBR pyrolysis.

The scope of the following research centers around developing an understanding of the mechanisms driving the formation of products during the pyrolysis (thermal decomposition in the absence of oxygen) of hydrocarbons, i.e. styrene butadiene rubber (SBR). Among those systems studied using FT-ICR were furan and 1,3-butadiene, both of which produce $C_3H_3^+$ upon electron impact of the neutral target gas. Although this work examines the formation of the phenyl cation, the scope of this research centers around developing an understanding of the gas phase reactions of $C_3H_3^+$ during the pyrolysis process and the implications of these reactions performed on a large scale.

Experimental

An IonSpec Omega 50 Fourier transform mass spectrometer (FTMS) based on the concept of ion cyclotron resonance was employed for the

experiments described in this report. Fundamental principles of FT-ICR and its function in gas phase ion-molecule reaction studies have been discussed in previous articles (21,22,23,24). The Omega 50 FTMS instrument uses a Walker Scientific resistive electromagnet which was set with a magnetic field strength of 1.03 T. Samples were introduced through a Varian Series 951 leak valve into a single vacuum chamber. Background pressure was maintained at 8 x 10^{-10} torr using a Balzers 330 liter/second turbomolecular pump backed by an Alcatel direct drive roughing pump. Pressures were monitored using a Bayard Alpert ionization gauge, with average experimental pressures set between 2.0-3.0 x 10^{-7} torr. The temperature was monitored using a calibrated thermocouple attached to the vacuum chamber and the neutral gases were allowed to equilibrate prior to kinetic measurements. Ionization followed a 20 ms electron beam with ion current set between 1.2-1.5 μA and electron energy of 60 eV. Experimental parameters and data acquisition were controlled using the IonSpec Omega System. Translational energy achieved through a radiofrequency (rf) excitation burst was calculated using the equation

$$T_{xy} = \frac{q^2 E^2 t^2}{8M} \qquad (3)$$

where $T_{x\text{-}y}$ represents the translational energy of the ion in joules, q represents the charge of one electron in coulombs, E represents the amplitude of the excitation burst in volts per meter, t represents the width of the excitation burst in seconds, and M represents the mass of the ion in kilograms per atom (22, 23). The value obtained for

the translational energy imparted to the ion was then used to calculate the orbital radius of the ion using the equation

$$r = \sqrt{\frac{t_{x-y}m}{4.823x10^{7}B^{2}}} \qquad (4)$$

where r represents the orbital radius of the ion, t_{x-y} represents the translational energy imparted to the ion in electron volts, k is a constant, and B represents the magnetic field strength in tesla (25,26). Values for the excitation time required for the resonant ejection of the molecular ion of furan was obtained and compared to the dimensions of the analyzer cell.(27). This data was used to calibrate the amplitude of the rf ejection fields used.

Results and Discussion

Formation of the phenyl cation. The gas phase reaction of $C_3H_3^+$ with neutral furan shows the formation of the phenyl cation (m/z 77) as well as the molecular ion (m/z 68) by charge exchange with the neutral target gas (Fig 1). Observation of time plot data shows only a portion of the $C_3H_3^+$ population reacting away to form these products, which is consistent with the observation

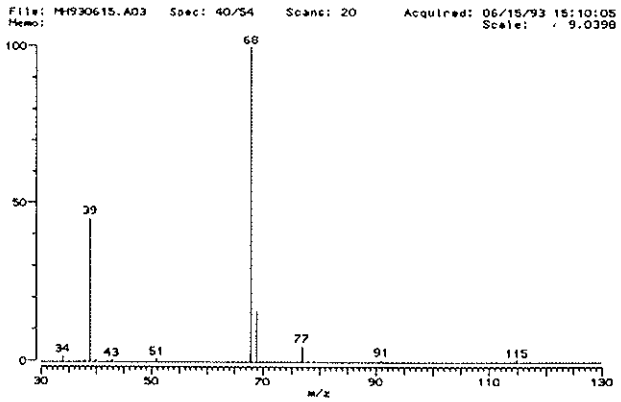

Figure 1: Mass spectrum of ion-molecule reaction products of furan.

of two stable isomeric populations of $C_3H_3^+$ produced in the gas phase (Fig 2). Research done by Eyler shows that the reactive portion of $C_3H_3^+$ is the propargyl, or linear form (2,3,4).

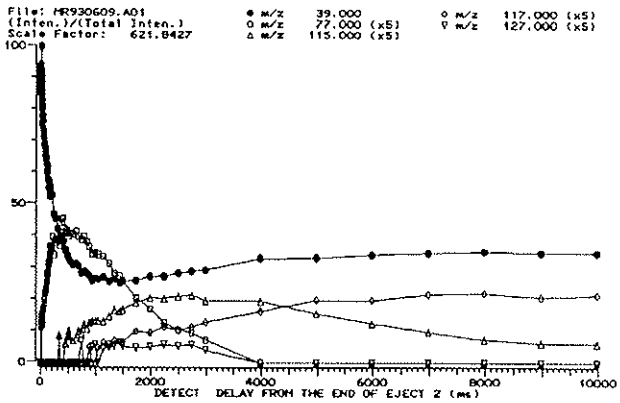

Figure 2: Time plot of l-C3H3+ reaction with furan showing formation of phenyl cation (m/z 77).

Isolation of $C_3H_3^+$ by ejecting all other ions from the cell using rf ejection sweeps enabled the reaction of the *l*-$C_3H_3^+$ to be observed more closely. It was determined that *l*-$C_3H_3^+$ reacts with neutral furan in reaction 4 to produce $C_6H_5^+$ (m/z 77), which reacts with neutral furan to form products of m/z 115, 117, 127 (Fig 2).

$$C_3H_3^+ + C_4H_4O \rightarrow [C_7H_7O]^+ \rightarrow C_6H_5^+ + CH_2O \qquad (4)$$

Formation of the intermediate condensation product, $C_7H_7O^+$ (m/z 107), from the above reaction could only be observed at high pressure ($>1 \times 10^{-3}$ torr) obtained using a pulse valve. In this experiment, *l*-$C_3H_3^+$ was isolated off the leak valve and neutral furan was pulsed into the trapping cell after a 20 ms electron beam. A stable $C_7H_7O^+$ intermediate was observed as a result of the reaction. It was concluded that the higher collision rate achieved at the higher pressure acted to stabilize the otherwise unstable intermediate by removing internal energy upon collision with the pulsed neutral gas. At

low pressure (~2 x 10^{-7} torr), the collision rate is not sufficient enough to cool the excited internal state of the intermediate resulting from the exothermic reaction, resulting in fragmentation to the $C_6H_5^+$ cation.

Rate coefficients for the appearance and disappearance of $C_6H_5^+$ in reaction 4 were determined at pressures of 9.5 x 10^{-8}, 1.8 x 10^{-7} torr and 5.6 x 10^{-7} torr. (Table I). Because the instrument maintains a constant pressure of the neutral during the reaction, a bimolecular rate law according to equation 5 below:

$$\text{rate} = k[A][B] \qquad (5)$$

where A and B are the concentrations of the reactant ion and the neutral, respectively, can be simplified according to a pseudo-first order reaction shown below:

$$\text{rate} = k'[A] \qquad (6)$$

where k' represents the product of the rate constant k and the concentration of the neutral. Based on a steady state approximation, the rate constant k' can be determined

Table I

Pressure(torr)	k'(appearance m/z 77)	k'(disappearance m/z 77)
9.5×10^{-8}	.00024	.00006
$*3.1 \times 10^{-9}$	$**7.8 \times 10^{-14}$	$**1.9 \times 10^{-14}$
1.8×10^{-7}	.00043	.00012
$*5.8 \times 10^{-9}$	$**7.4 \times 10^{-14}$	$**2.1 \times 10^{-14}$
5.6×10^{-7}	.00094	.00035
$*1.8 \times 10^{-9}$	$**5.2 \times 10^{-14}$	$**1.9 \times 10^{-14}$

values for k' were calculated as follows:
$\ln(1-A/A_o)/t = k'$
*denotes concentration in molecules/cm^3
note: 3.23×10^{16} molecules/cm^3torr

**denotes value for k in cm^3/(molecules × ms) based on a bimolecular rate law calculated

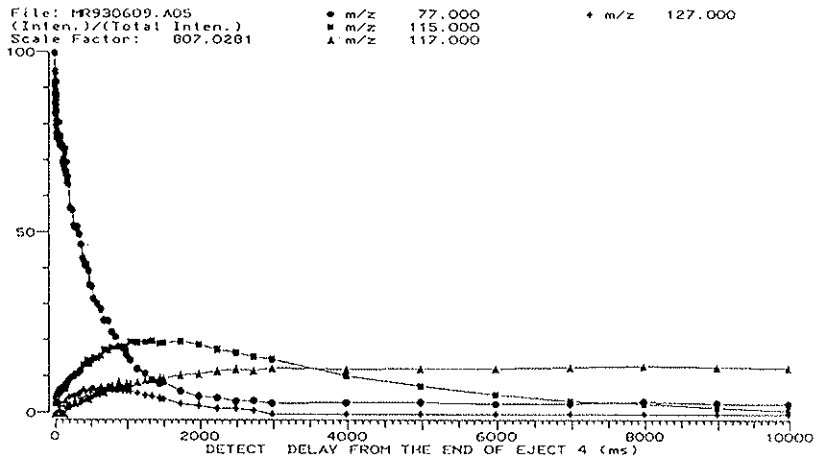

Figure 3: Time plot of reaction of phenyl cation with furan.

by equation 7 below:

$$\mathrm{Ln}(A/A_o) = k't \qquad (7)$$

The rate constant k can then be determined by dividing by the concentration of the neutral gas. The concentration of the neutral gas (Table I) in molecules/cc (number density) can be evaluated from the pressure by noting that there are 3.23×10^{16} molecules cc^{-1} $torr^{-1}$ (18). It is important to note that this large rate constant is consistent with reaction rates observed by Eyler for the reactions of *l*-$C_3H_3^+$ and acetylene (3) and is approximately equal to the Langevin and ADO collision rates.

In order to verify the structure of $C_6H_5^+$ as the phenyl cation, reaction rates and the formation of products from the $C_3H_3^+$ reaction with neutral furan were compared to the reaction of the phenyl cation produced from iodobenzene with neutral furan (Fig 3). Both the product distribution formed from the reaction of the phenyl cation produced from E.I. of iodobenzene with neutral, as well as the reaction rates were consistent with that previously observed between $C_6H_5^+$ and furan.

Because the precursor for the phenyl cation in the above experiment was iodobenzene, neutral iodobenzene would be present in the analyzer cell along with neutral furan. Therefore, a reaction was observed between the phenyl cation and neutral iodobenzene in order to gain background on the product formation from this reaction alone. Results of this reaction showed no production of 115, 117 or 127 (Fig 4). A

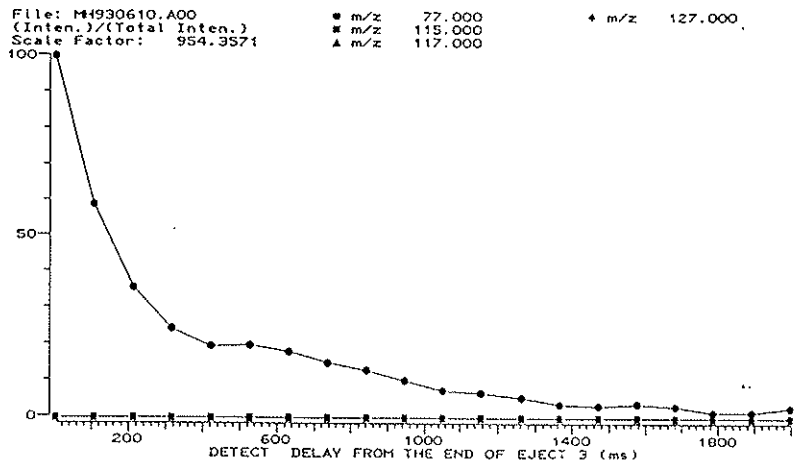

Figure 4: Time plot for reaction of phenyl cation with iodobenzene.

previous reaction of the phenyl cation with iodobenzene was performed by Duhachek (24) which further confirmed the results presented here.

Reactions of c-$C_3H_3^+$.

In order to investigate the reaction barrier existing between the two isomeric forms of $C_3H_3^+$, an experiment was performed in which the *c*-$C_3H_3^+$ isomer was isolated and allowed to react with the neutral furan. This was accomplished by delaying the isolation sequence 2500 ms, thus allowing ample time for the reactive propargyl isomer to be consumed (Fig 5). The results of this experiment show no production of the phenyl cation and consequently a very minor decrease in the amount of *c*-$C_3H_3^+$ present (Fig 6).

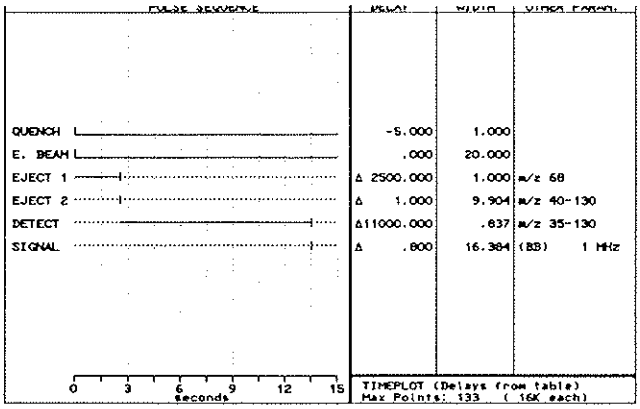

Figure 5: Pulse sequence for c-C3H3+ with furan.

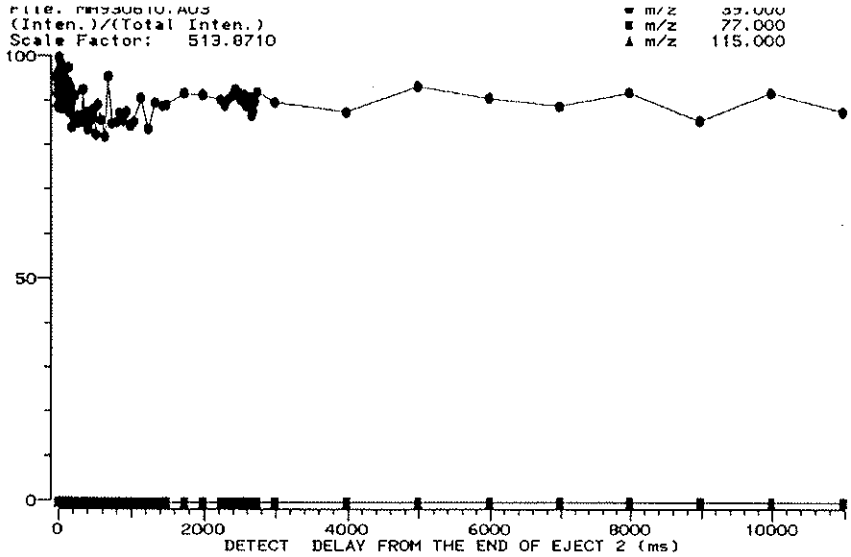

Figure 6: Time plot for reaction of c-C3H3+ with furan showing no production of the phenyl cation.

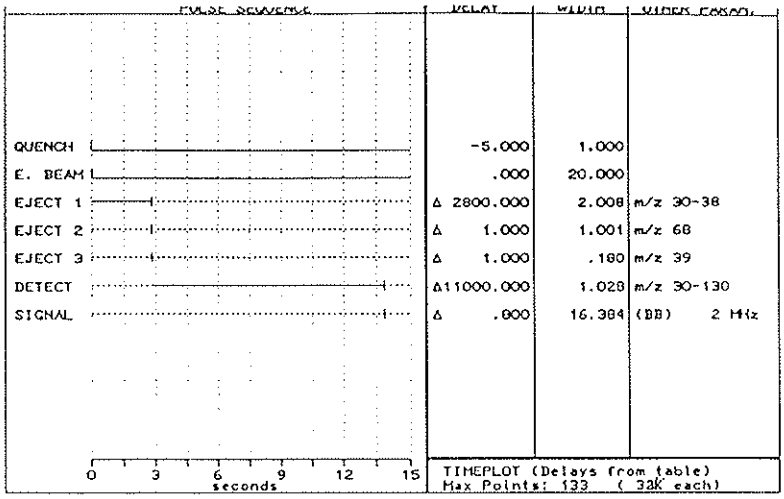

Figure 7: Pulse sequence for reaction in which c-C3H3+ is given a rf burst of energy.

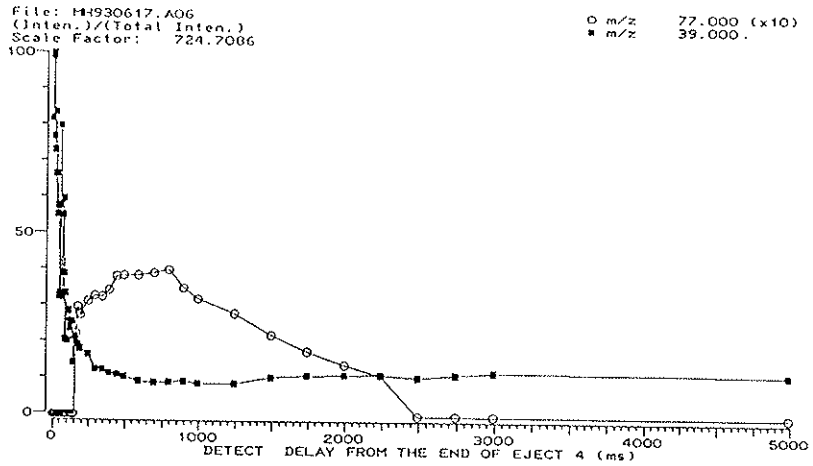

Figure 8: Time plot of reaction in which c-C3H3+ is given a rf burst of energy.

It was postulated that a reaction may be forced to occur by increasing the translational energy of the *c*-$C_3H_3^+$, thus causing it to internalize more energy upon collision with the furan neutral. This was done by repeating the previous experiment with a quick rf excitation burst on the isolated *c*-$C_3H_3^+$ (Fig 7). A time plot of this reaction reveals the formation of $C_6H_5^+$ similar to that of the reaction between the propargyl isomer and furan (Fig 2, 8). The threshold energy required to force the reaction was further studied by imparting increasing amounts of translational energy to the *c*-$C_3H_3^+$ through increasing rf excitation burst widths (Fig 9). A time plot of these various widths shows optimum production of the phenyl cation between widths of about .18 ms and .22 ms (Fig 10). These values equate to 8 x 10^{-17} joules and 1.2 x 10^{-16} joules (500 eV - 740 eV), respectively,

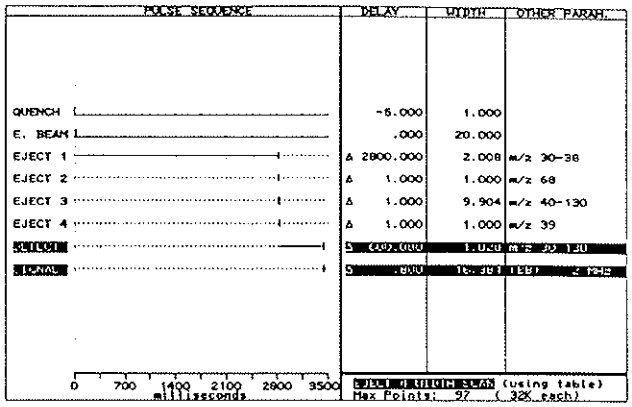

Figure 9: Pulse sequence for reaction in which increasing amounts of translational energy were imparted to c-C3H3+.

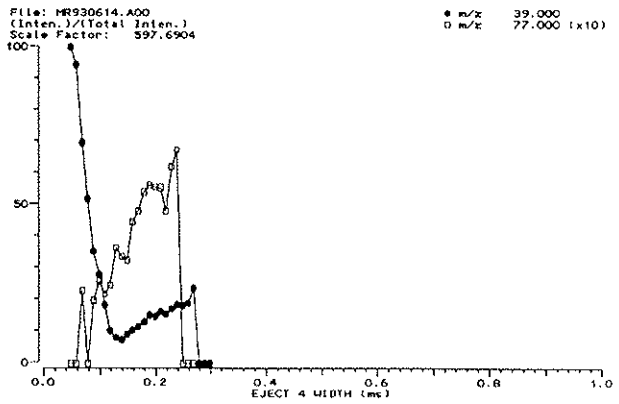

Figure 10: Time plot showing energy required to overcome reaction barrier of c-C3H3+.

of translational energy acquired by the *c*-$C_3H_3^+$ cation using equation 3. Extrapolating the time plot in figure ten back to the initial appearance of $C_6H_5^+$ cation gives the minimum amount of translational energy required to induce a reaction between the *c*-$C_3H_3^+$ and neutral furan . The appearance of $C_6H_5^+$ cation at 40 μs. corresponds to a threshold energy for the reaction of 19 ev. This observation is consistent with the high energy barrier calculated for the interconversion of the two forms of the $C_3H_3^+$ cation.

The values obtained for translational energy were studied further by evaluating whether the orbital radius acquired by the ion as a result of the increased translational energy was reasonable for the diameter of the analyzer cell (.05 m). The range for the orbital radius was .0076 to .024 meters. Therefore, it can be noted that the values obtained are within the maximum orbital radius (.025 m) possible for an ion according to the dimensional limits of the cell.

Deuterium labeling experiments.

In order to postulate a mechanism for reaction 4, deuterium labeling experiments were performed using deuterated furan (3).

Upon electron impact of deuterated furan, $C_3D_3^+$ (m/z 42) was produced as a fragment. Using various ejection sweeps, a reaction was performed in which $C_3D_3^+$ was isolated. Target gases in the experiment were both deuterated and protonated furan. The major $C_6H_xD_y^+$ (where x and y sum to 5) were of m/z 79, 80, 82 as shown by reactions 8, 9, and 10, respectively (Fig 11).

$$C_3D_3^+ + C_4H_4O \rightarrow C_6H_3D_2^+ + CHDO \qquad (8)$$

$$C_3D_3^+ + C_4H_4O \rightarrow C_6H_2D_3^+ + CH_2O \qquad (9)$$

$$C_3D_3^+ + C_4D_4O \rightarrow C_6D_5^+ + CD_2O \qquad (10)$$

As can be noted from the above reactions, the only reaction pathway for the production of m/z 82 is through reaction 10 in which all hydrogens, as observed in reaction 4, are replaced by deuterium. Production of ions of m/z 79 and 80, however, may also proceed through reactions 11 and 12, respectively.

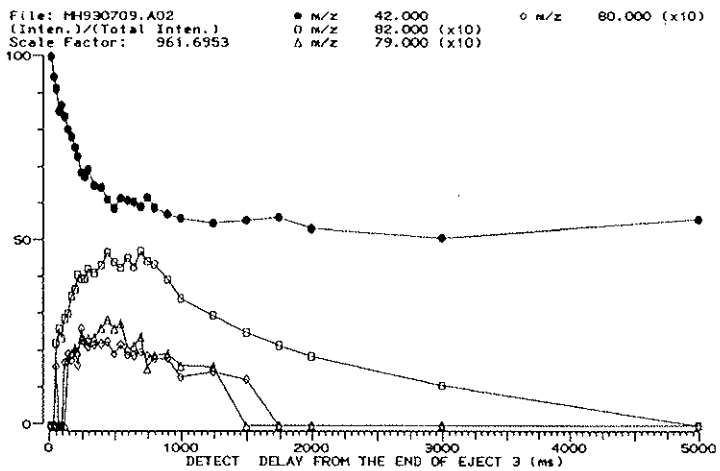

Figure 11: Time plot of $C_3D_3^+$ reaction with C_4D_4O and C_4H_4O showing production of ions of m/z 79, 80, 82.

$$C_3H_3^+ + C_4D_4O \rightarrow C_6H_3D_2^+ + CD_2O \qquad (11)$$

$$C_3H_3^+ + C_4D_4O \rightarrow C_6H_2D_3^+ + CHDO \qquad (12)$$

Comparison of reaction rate time plots for ions of m/z 79 and 80 are identical (Fig 12). Furthermore, the sum of the intensities of these two plots over time is very similar to the intenity of the intensity/time plot for m/z 82 (Fig 12).

$C_3H_3^+$ and $C_3D_3^+$ reactions with 1, 3-butadiene were also observed. Upon elecron impact of 1, 3-butadiene, $C_3H_3^+$ was observed as a fragment ion. Once again two population of $C_3H_3^+$ were observed, the propargyl and the cyclopropenyl isomers. A reaction between $C_3H_3^+$ and 1, 3-butadiene again revealed the formation of $C_6H_5^+$.

$C_3D_3^+$ reactions with 1, 3-butadiene neutral produced ions of m/z 79 and 80 with similar rates of appearance compared to that in the experiments involving the furan neutral.

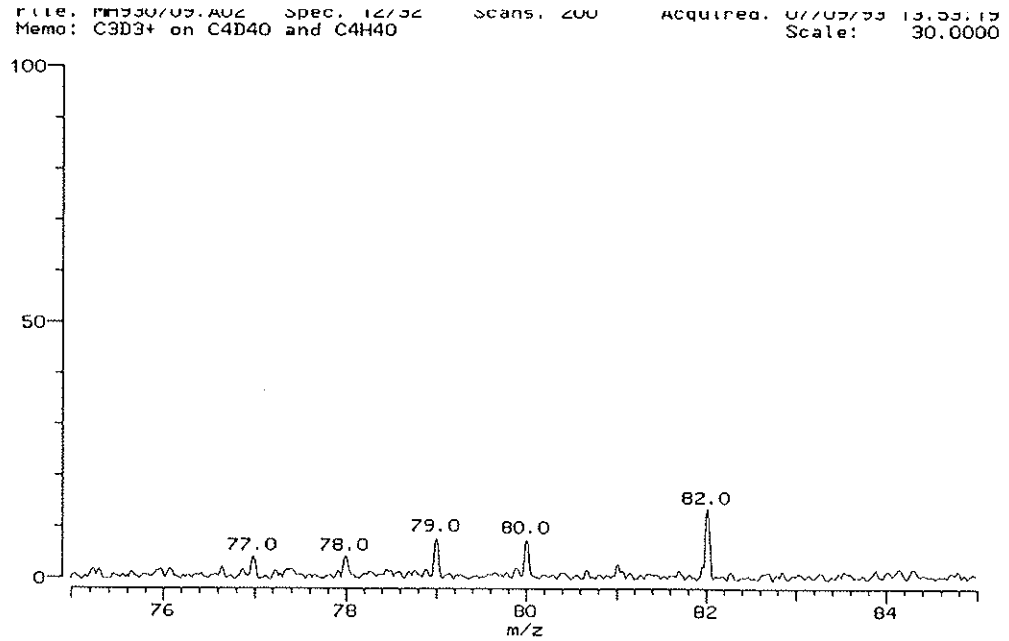

Figure 12: Mass spectrum showing products from the reaction of $C_3D_3^+$ with C_4D_4O and C_4D_4O.

Conclusion

The reactions of $C_3H_3^+$ with low molecular weight hydrocarbons, such furan and 1, 3-butadiene have been extensively studied. The results of these reactions show many similarities regarding the formation of $C_6H_5^+$. Results from deuterium labeling experiments are consistent with the idea that the formation of $C_6H_5^+$ (refer to equations 4, 8-12) is driven by one mechanism in which complete hydrogen scrambling occurs. This could happen by incorporation of all three carbons into the intermediate structure resulting in a seven member ring
intermediate.

Results from pulse valve experiments in which the $C_7H_7O^+$ intermediate was observed hold implications for experiments performed under high energy parameters, as in the pyrolysis of hydrocarbons. High energy environments may destabilize intermediates forcing fragmentation to aromatic products. Increased reaction times, as in large batch pyrolysis ovens, would then result in the formation of aromatic hydrocarbons before collection occurs.

Furthermore, this research has also shown how the *c*-$C_3H_3^+$ can be rendered reactive once it overcomes its energy barrier. Once again, the high energy parameters of pyrolysis may also enable the cyclic isomer to overcome this energy barrier, therefore causing reactions to occur involving the cyclic isomer as well as the propargyl isomer. Two theories may explain the mechanism by which the *c*-$C_3H_3^+$ is rendered reactive toward the neutral furan: *i)* A two collision reaction may occur in which one collision

results in rearrangement of the cyclic form to the linear form, and then a second collision results in the formation of the intermediate complex which then fragments to form the phenyl cation, or *ii)* an endothermic reaction may occur by which the cyclic form complexes with the neutral furan upon one collision, with possible simultaneous ring opening, and then proceeds to fragment to form the phenyl cation.

The pervasive nature of $C_3H_3^+$ suggests that its role in the pyrolysis of SBR tires is consistent with an ionic model. The rapid rate at which it reacts with the small conjugated dienes studied here further strengthens the idea of an ionic mechanism driving the formation of products during the pyrolysis process.

ACKNOWLEDGEMENT

We would like to express our gratitude for the funding provided by the Small Business Association, the Reuse Recycling and Technology Transfer Center, and the Graduate College of University of Northern Iowa

LITERATURE CITED

1. Calcote, H. F. *Combustion and Flame.* 1981. *42*, 215-242.

2.Wiseman, F. L.; Ozturk, F.; Zerner, M. C.; Eyler, J. R. *Int. J. of Chem. Kinet.* **1990**, *22*, 1189-1209.

3. Ozturk, F.; Baykut, G.; Moini, M.; Eyler, J. R. *J. Phys. Chem.* **1987**, *91*, 4360-4364.

4. Baykut, G.; Brill, F. W.; Eyler, J. R. *Combust. Sci. and Tech.* **1986**, *45*, 233-243.

5.Bowser, R. J.; Weinberg, F. J. *Combustion and Flame.* **1976**, *27*, 21-32.

6.Bowser, R. J.; Weinberg, F. J. *Combustion and Flame.* **1976**, *27*, 21-32.

7.Weiner, B.; Williams, C. J.; Heaney D. *J. Phys Chem.* **1990**, *94*, 7001-7007.

8.Ausloos, P. J.; Lias, S. G. *J. Am. Chem. Soc.* **1981**, *103*, 6505-6507.

9.Wu, C. H.; Kern, R. D. *J. Phys. Chem.* **1987**, *91*, 6291-6296.

10.Calcote, H. F.;Olson, D. B.; Keil, D. G. *Energy and Fuels* 1988, *2*, 494-504.

11.Groenewold, G. S.; Gross, M. L.; *J. Am. Chem. Soc.* **1984**, *106*, 6569-6575.

12.van Doorn, R.; Nibbering, N; Ferrer-Correia, A.J.V.; Jennings, K. R. *Org. Mass Spectrom.* **1978**, *13*, 729-732.

13.Radom, L.; Hariharan P. C.; Pople, J. A.; Schleyer, P. V. R. *J. Am. Chem. Soc.*, **1976**, *98*, 10.

14.Lossing, F. P. *Can. J. Chem.*, **1972**, *50*, 3973.

15.Wong, M. W.; Radom, L. *J. Am. Chem. Soc.*, **1989**, *111*, 6980.

16.Wingfield, Jr. et al. US Patent 4,515,659, 1985.

17.Pakdel, H.; Roy, C.; Aubin, H.; Jean, G.; Coulombe, S.; *Environ. Sci. Technol.* **1991**, *25*, 1646-1648.

18.Kopinke, F. D.; Zimmerman, G.; Ondruschka, B.; *Ind. Eng. Chem. Res.* **1987**, *26*, 2393-2397.

19.Klempier, N.; Binder, H.; *Anal. Chem.* **1983**, *55*, 2104-2106.

20.Rich, M. R.; Hammer, M. D.; Burrell, T.; Hanson, C. D. Manuscripts in preparation, University of Northern Iowa, 1993.

21.Hanson, C. D.; Kerley, E. L.; Russell, D. H. **Recent Developments in Experimental FT-ICR.** *Treatise on Analytical Chemistry*. Second Edition, Part 1, Volume 11, Chapter 2, **1989**, Ed. M. Bursey. J. Wiley Publ.

22.Gross, M. L.; Rempel, D. L. *Science*, **1984**, *226*, 261-268.

23.Hanson, C. D.; Kerley, E. L.; Castro, M. E.; Russell, D. H.; *Analytical Chemistry*. **1989**, *61* 2040-2046.

24.Burnier, R. C.; Freiser, B. S. *J. Chem Ed.* **1979**, *56*, 687-692.

25.Beauchamp, J. L. *Ann. Rev. Phys. Chem.* **1971**, *22*, 527-561.

26.Kerley, E. L.; Russell, D. H.; *Analytical Chemistry*. **1989**, *61*, 53-57.

27.Beauchamp, J. L.; Armstrong, T. J. *Rev. Sci. Instrum.* **1969**, *40*, 123-128.